Published in final edited form as:

Biol Psychiatry. 2014 April 15; 75(8): 623–630. doi:10.1016/j.biopsych.2013.01.008.

Circuit-selective striatal synaptic dysfunction in the *Sapap3* knockout mouse model of obsessive-compulsive disorder

Yehong Wan[1], **Kristen Ade**[1], **Zachary Caffall**[1], **M. Ilcim Ozlu**[3], **Cagla Eroglu**[2,3], **Guoping Feng**[4], and **Nicole Calakos**[1,2]

[1]Department of Medicine, Division of Neurology, Duke University, Durham, North Carolina 27710, USA

[2]Department of Neurobiology, Duke University, Durham, North Carolina 27710, USA

[3]Department of Cell Biology, Duke University, Durham, North Carolina 27710, USA

[4]Department of Brain and Cognitive Sciences, McGovern Institute for Brain Research, MIT, Cambridge, MA 02139, USA

Abstract

Background—SAP90/PSD-95-associated protein 3 (SAPAP3, also DLGAP3 or GKAP3) is an excitatory postsynaptic protein implicated in the pathogenesis of obsessive-compulsive behaviors. In mice, genetic deletion of *Sapap3* causes obsessive-compulsive disorder (OCD)-like behaviors that are rescued by striatal expression of *Sapap3*, demonstrating the importance of striatal neurotransmission for the OCD-like behaviors. In the striatum, there are two main excitatory synaptic circuits, corticostriatal and thalamostriatal. Neurotransmission defects in either or both of these circuits could potentially contribute to the OCD-like behaviors of *Sapap3* knockout (KO) mice. Previously we reported that *Sapap3* deletion reduces corticostriatal AMPA-type glutamate receptor (AMPAR)-mediated synaptic transmission.

Methods—Whole-cell electrophysiological recording techniques in acute brain slices were used to measure synaptic transmission in the corticostriatal and thalamostriatal circuits of *Sapap3* KO mice and littermate controls. Transgenic fluorescent reporters identified striatopallidal and striatonigral projection neurons. SAPAP isoforms at corticostriatal and thalamostriatal synapses were detected using immunostaining techniques.

Results—In contrast to corticostriatal synapses, thalamostriatal synaptic activity is unaffected by *Sapap3* deletion. At the molecular level, we find that another SAPAP family member, SAPAP4, is present at thalamostriatal, but not corticostriatal synapses. This finding provides a molecular rationale for the functional divergence we observe between thalamic and cortical striatal circuits in *Sapap3* KO mice.

Conclusion—These findings define the circuit-level neurotransmission defects in a genetic mouse model for OCD-related behaviors, focusing attention on the corticostriatal circuit for

Correspondence should be addressed to Nicole Calakos, Box 2900, Duke University Medical Center, Durham, NC 27710. nicole.calakos@duke.edu.

Financial Disclosures

The authors report no biomedical financial interests or potential conflicts of interest.

mediating the behavioral abnormalities. Our results also provide the first evidence that SAPAP isoforms may be localized to synapses according to circuit-selective principles.

Keywords

obsessive-compulsive disorder; SAPAP3; striatum; thalamostriatal; corticostriatal; GKAP; DLGAP3

Introduction

SAPAPs (also known as guanylate kinase-associated proteins, GKAPs or DLGAPs) are a family of postsynaptic scaffold proteins that are unique to excitatory synapses and well poised to influence synaptic activity of ionotropic and metabotropic glutamate receptors by virtue of their interaction with proteins such as PSD-95 and Shank (1-6). Loss of SAPAP3, the only SAPAP highly expressed in striatum, causes pathological grooming and anxiety-like behaviors in mice suggesting relevance to obsessive-compulsive disorder (OCD) (7). *Sapap3* KO mice show excessive self-grooming and develop facial lesions. Anxiety-like behaviors as detected in the elevated zero maze, open field test, and light-dark emergence assay are also present. Predictive validity of this model is indicated by the finding that the entire constellation – self-grooming, facial lesions and anxiety-like behaviors – is alleviated by chronic (5 d.) treatment with a selective serotonin reuptake inhibitor, a first-line treatment for OCD. More recent evidence from human genetic studies also supports a role for SAPAPs in obsessive-compulsive behaviors (8-10).

Human neuroimaging studies of OCD have identified abnormalities throughout the cortico-striato-thalamo-cortical circuitry (11). However, determining which regions may be the origins of abnormal activity and which regions are driven abnormally as a consequence of a proximal insult is difficult to elucidate in this experimental approach. In *Sapap3* KO mice, the circuit basis for the OCD-like behaviors has been localized to the striatum through rescue experiments in which lentiviral-mediated expression of *Sapap3* limited to the striatum was sufficient to prevent the behavioral defects (7). Given the striatal-dependent OCD-like behaviors of *Sapap3* KO mice, a detailed understanding of the striatal circuit changes in *Sapap3* KO mice can identify potential circuit mechanisms for behaviors relevant to OCD. In recent work, we found that *Sapap3* deletion reduces corticostriatal AMPAR-mediated synaptic transmission (6), but the integrity of thalamostriatal transmission was not examined.

The striatum, the input nucleus of the basal ganglia, receives excitatory afferents from both cerebral cortex and thalamus. Corticostriatal and thalamostriatal circuits differentially contribute to behavior (12, 13). Corticostriatal and thalamostriatal synapses onto medium spiny neurons (MSNs) are also known to have different anatomical and physiological properties (14-17). Finally, although ultrastructural properties of postsynaptic spines have been compared between corticostriatal and thalamostriatal synapses (18), little is known about molecular differences in the postsynaptic density which may give rise to such differences.

In this study, we examined the integrity of thalamostriatal synaptic transmission in striatonigral and striatopallidal MSNs of *Sapap3* KO mice. Surprisingly, our results show that *Sapap3* deletion does not affect thalamostriatal AMPAR synaptic activity. Consistent with this circuit-selective functional difference (i.e. impaired corticostriatal and preserved thalamostriatal activity), we find that another isoform, SAPAP4 is present at thalamostriatal synapses, but not corticostriatal synapses. This finding reveals for the first time a postsynaptic molecular specificity in MSNs that distinguishes two striatal inputs, while the

associated circuit-selective functional impairment of excitatory synaptic transmission in *Sapap3* KO mice advances our circuit-level understanding of OCD-like behaviors.

Materials and Methods

Brain slice preparation

Animal procedures were performed according to protocol approved by the Institutional Animal Care and Use Committee of Duke University. Generation of *Sapap3* KO, *Drd1a*-tdTomato$^{(tg/+)}$ transgenic, and *Drd2*-EGFP$^{(tg/+)}$ transgenic mice has been previously described (7, 19, 20). From littermate pairs of P21–25 *Sapap3* wild-type (WT) and KO mice hemizygous for *Drd1a*-tdTomato and/or *Drd2*-EGFP transgenes, acute coronal or parahorizontal brain slices (300 μm thickness) were obtained as previously described (6, 14). All experiments were performed with experimenter blinded to *Sapap3* genotype.

Electrophysiology

Recordings were obtained at room temperature (23-25°C). $GABA_A$ receptors were blocked by 50 μM picrotoxin (Sigma-Aldrich). Glycine (1 μM) was present in NMDA-type glutamate receptor (NMDAR)-mediated excitatory postsynaptic current (EPSC) experiments. According to their axonal projection patterns, striatal MSNs are classified into two types, striatonigral (SN) and striatopallidal (SP) MSNs (21). Since the two types of MSNs have different synaptic properties (22), transgenic mice expressing fluorescent marker proteins were used to distinguish SN and SP MSNs (20). Whole-cell patch-clamp recordings were made as described in (6).

Cortical afferents were evaluated using coronal slices with stimulating electrode placed in corpus callosum adjacent to dorsolateral striatum. Thalamic afferents were evaluated using parahorizontal slices with stimulating electrode placed in thalamus close to medial border of the thalamic reticular nucleus (14). To evoke EPSCs, 150-μs duration stimuli were delivered at 0.05 Hz through a bipolar electrode made of monopolar tungsten electrodes (FHC). Paired-pulse ratios were calculated by the ratio of the peak of the second EPSC to the peak of the first EPSC using a 50-ms inter-stimulus interval. AMPAR/NMDAR ratio was calculated by the ratio of the peak of the EPSC at -70 mV to the magnitude of the EPSC at +40 mV at 60 ms following stimulation.

Miniature EPSCs (mEPSCs) were recorded in 1 μM tetrodotoxin (TTX; Tocris) and analyzed using Mini Analysis Program software (Synaptosoft). Quantal EPSCs (qEPSCs) during the asynchronous phase of evoked release were recorded in standard ACSF containing 0 mM Ca^{2+}, 2 mM Sr^{2+} and 50 uM AP-5 (Tocris). AMPAR-mediated qEPSCs were analyzed during a 300 ms period beginning 50 ms after each stimulus. For mEPSC and qEPSC analysis, threshold amplitude for detection of events was 5 pA.

Primary co-cultures and immunostaining

Corticostriatal and thalamostriatal co-cultures were prepared from P0 *Sapap3* WT mice as previously described (5) with the modification that thalamic tissue was used for thalamostriatal cultures and plated in a ratio of 1:1 of thalamic and striatal cells. On DIV 13-14, cultures were fixed and immunostained as previously described (5). Primary antibodies were: anti-vGluT1 mouse monoclonal antibody (1:400; Synaptic Systems 135511), anti-vGluT2 guinea pig polyclonal antibody (1:200; Synaptic Systems 135404), anti-SAPAP4 rabbit polyclonal antibody (1:400) (3), and anti-DARPP32 rat monoclonal antibody (1:60; R&D Systems MAB4230). Affinity-purified SAPAP4 antibody was generated against a His-tagged fusion protein encoding SAPAP4 amino acids 612-689 as previously described (3). SAPAP4 isoform-selectivity was demonstrated previously using

Western blot analysis to discriminate SAPAP isoforms by molecular weight (3). Primary antibody incubations were performed at 4°C overnight. Appropriate secondary antibodies (Alexa Fluor 488-conjugated goat anti-mouse IgG, Alexa Fluor 568-conjugated goat anti-guinea pig IgG, Alexa Fluor 488-conjugated goat anti-guinea pig IgG, Alexa Fluor 568-conjugated goat anti-rabbit IgG, 1:800, Molecular Probes; Cy5-conjugated donkey anti-rat IgG, 1:200, Jackson ImmunoResearch) were incubated for 2 hours at room temperature after washing primary antibody incubation solution and re-blocking. Images were obtained using a 40×/1.3 oil objective on an LSM 510 confocal microscope (Zeiss). Alexa Fluor 488 dye was excited with a 488 nm Argon laser. Alexa Fluor 568 dye was excited with a 561 nm diode laser. Cy5 dye was excited with a 633 nm HeNe laser. No cross talk between channels was detected under these settings. MetaMorph software (Molecular Devices) was used for analysis. MSN dendrites were identified by DARPP32 staining (indicator of medium spiny neurons) and selected for analysis if they did not have other dendrites overlying. The percentage of colocalized area was defined as the percentage of vGluT1 or vGluT2-positive area that was also labeled with SAPAP4.

Brain slice immunostaining

Immunostaining in brain slices was performed as previously described (23). Briefly, P21-25 mice were perfused with Tris-buffered saline (TBS) followed by 4% paraformaldehyde (PFA). Brains were immersed in 4% PFA/30% sucrose solution overnight at 4°C. Tissue was embedded in a 2:1 mixture of 20% sucrose in phosphate-buffered saline (PBS):OCT (Tissue-Tek, Cat. No: 4583) in PBS, and cryo-sectioned (coronal, 20 μm). Brain slices were incubated for 72 hours at 4°C with primary antibodies: guinea pig anti-vGluT2 antibody (1:2500; Millipore, AB5905) and rabbit anti-SAPAP4 antibody (1:400) (3). Secondary Alexa-488-conjugated goat anti-guinea pig IgG (1:500; Invitrogen) and Alexa 594-conjugated goat anti-rabbit IgG (1:500; Invitrogen) antibodies were used for detection of primary antibodies. Slides were mounted in Vectashield (Vector Laboratories Inc.) with DAPI (i.e. 4',6-diamidino-2-phenylindole) and imaged on a Leica SP5 confocal laser-scanning microscope using a 63× oil objective. For each tissue slice, serial optical sections at 0.33 μm intervals were acquired over a total depth of 5 μm for a total of 15 optical sections. Maximum intensity projections (MIPs) were generated from 3 consecutive sections yielding MIPs representing 1μm of depth each. To analyze co-localization of vGluT2- and SAPAP4-postive puncta, MIPs were quantified using the Puncta Analyzer program in ImageJ 1.26 (23). The percentage of colocalized area was defined as the percentage of SAPAP4 area that was also labeled with vGluT2.

Statistical analysis

All data presented as mean ± standard error of the mean. Error bars indicate standard error of the mean. Group results were compared by *t*-test, ANOVA, or Mann-Whitney test. Asterisk indicates a *p*-value of < 0.05.

Results

In striatopallidal MSNs, circuit-selective analysis is necessary to reveal defect in quantal synaptic events

Circuit-selective studies to examine thalamostriatal transmission were prompted by finding that SP MSNs had discordant effects of *Sapap3* deletion on miniature and evoked EPSCs. In prior studies, we demonstrated that *Sapap3* deletion reduced AMPAR-mediated evoked EPSCs in both SN and SP MSNs (6). In SN MSNs, this was accompanied by a significant reduction in the frequency of mEPSC events (6). However, in SP MSNs, we show here that mEPSCs are unaffected by *Sapap3* deletion. No significant differences were detected in either frequency or amplitude (frequency: WT, 4.1 ± 0.4 Hz, 22 cells; KO, 3.7 ± 0.3 Hz, 22

cells; $p = 0.416$, *t*-test; Figure 1A, B; amplitude: WT, -14.3 ± 0.3 pA, 22 cells; KO, -15.2 ± 0.4 pA, 22 cells; $p = 0.152$, Mann-Whitney; Figure 1A, C).

To investigate the reason for this incongruence, we considered whether differences in the source of afferent fibers contributing to each type of synaptic response (i.e. miniature vs. evoked) could explain our observations. Evoked EPSCs (eEPSCs) are biased towards inputs activated by the experimenter's stimulating electrode, whereas mEPSC events reflect all inputs and are not dependent upon electrode stimulation. To specifically evaluate quantal events that come from the population of synapses activated in the evoked EPSC experiments, we analyzed quantal EPSCs elicited by evoking EPSCs in the presence of Sr^{2+} (in place of Ca^{2+}) (14, 24). In the presence of Sr^{2+}, action potential-dependent presynaptic neurotransmitter release events are significantly prolonged resulting in asynchronous quantal events after the initial synchronous release. Using this approach, we first validated that qEPSC event analysis could detect an impairment in event frequency as we previously observed for mEPSCs in *Sapap3* KO SN neurons (6). Upon cortical stimulation, we found that qEPSC frequency was reduced in *Sapap3* KO SN MSNs (WT, 45.5 ± 3.8 Hz, 13 cells; KO, 34.9 ± 3.0Hz, 13 cells; $p = 0.038$, *t*-test; Figure 2A-D). These results are consistent with our published findings of both a reduced mEPSC frequency and reduced corticostriatal evoked EPSC amplitudes in *Sapap3* KO SN MSNs (6).

We then asked whether qEPSC frequency deriving from cortical afferents was reduced in SP MSNs of *Sapap3* KO mice. In SP MSNs, the frequency of qEPSCs elicited by cortical stimulation was reduced in *Sapap3* KO mice (frequency: WT, 33.6 ± 3.9 Hz, 13 cells; KO, 20.9 ± 3.4 Hz, 13 cells; $p = 0.022$, *t*-test; amplitude: WT, -19.4 ± 0.6 pA, 13 cells; KO, -17.6 ± 0.9 pA, 13 cells; $p = 0.061$, Mann-Whitney; Figure 2E-G). These results reveal that corticostriatal synaptic quantal events are impaired in SP MSNs. These results are consistent with our published finding of reduced SP MSN corticostriatal eEPSCs in *Sapap3* KO mice (6) and are in contrast to our mEPSC analysis, a measure that is not circuit-selective (Figure 1A-C).

AMPAR activity at thalamostriatal synapses is unaffected by *Sapap3* deletion

The discordant results between mEPSCs and eEPSCs of SP MSNs raise the possibility that a subpopulation of excitatory synapses onto MSNs might be unaffected by *Sapap3* deletion. If present, the contribution of such a synaptic population to mEPSCs could obscure detection of the impairment among corticostriatal synapses. The striatum has two major sources of excitatory afferents: cortex and thalamus. To test whether *Sapap3* deletion affected thalamostriatal synapses, we employed a parahorizontal slice preparation that allows selective activation of these inputs (Figure 3A) (14, 16). Consistent with our goal of stimulating a distinct subset of MSN inputs, paired-pulse ratios (PPRs) of evoked EPSCs resulting from thalamic and cortical stimulation differed (SP MSNs: cortical, 1.06 ± 0.03, 23 cells; thalamic, 0.66 ± 0.05, 15 cells; $p < 0.001$, Mann-Whitney; Figure 3B; SN MSNs: cortical, 0.98 ± 0.03, 29 cells; thalamic, 0.73 ± 0.06, 19 cells; $p < 0.001$, Mann-Whitney; Figure 3C) and were similar to values previously reported in mouse for corticostriatal and thalamostriatal synapses in these two MSN populations (14).

Using the approach we employed at corticostriatal synapses, we analyzed qEPSCs at thalamostriatal synapses in SP and SN MSNs from *Sapap3* KO and WT mice. In both SP and SN MSNs, we found no significant difference between WT and *Sapap3* KO mice in thalamic qEPSC frequency or amplitude (frequency – SP MSNs: WT, 14.4 ± 1.5 Hz, 11 cells; KO, 12.7 ± 1.2 Hz, 12 cells; $p = 0.378$, *t*-test; Figure 3D, E; SN MSNs: WT, 19.1 ± 2.2 Hz, 13 cells; KO, 20.0 ± 2.1 Hz, 15 cells; $p = 0.765$, *t*-test; Figure 3G, H; amplitude – SP MSNs: WT, -17.8 ± 0.8 pA, 11 cells; KO, -19.2 ± 0.7 pA, 12 cells; $p = 0.268$, Mann-Whitney; Figure 3D, F; SN MSNs: WT, -21.1 ± 0.9 pA, 13 cells; KO, -21.2 ± 0.8 pA, 15

cells; $p = 0.782$, Mann-Whitney; Figure 3G, I). Likewise, AMPAR/NMDAR ratios of thalamic eEPSCs in SP and SN MSNs of *Sapap3* KO mice were normal (SP MSNs: WT, 3.22 ± 0.35, 16 cells; KO, 3.38 ± 0.30, 16 cells; $p = 0.429$, Mann-Whitney; Figure 3J; SN MSNs: WT, 2.76 ± 0.20, 19 cells; KO, 3.24 ± 0.31, 16 cells; $p = 0.246$, Mann-Whitney; Figure 3L). Finally, thalamostriatal PPRs were normal in both SP and SN MSNs of *Sapap3* KO mice (SP MSNs: WT, 0.66 ± 0.05, 15 cells; KO, 0.57 ± 0.05, 16 cells; $p = 0.236$, Mann-Whitney; Figure 3K; SN MSNs: WT, 0.73 ± 0.06, 19 cells; KO, 0.73 ± 0.06, 16 cells; $p = 0.741$, Mann-Whitney; Figure 3M). These results indicate that *Sapap3* deletion has a circuit-selective effect on excitatory synaptic transmission in both SP and SN MSNs – decreasing corticostriatal, but not thalamostriatal responses.

Molecular heterogeneity of SAPAPs at corticostriatal and thalamostriatal synapses

The most straightforward explanation for the differential alteration of striatal synapses by *Sapap3* deletion in thalamic and cortical circuits is that another SAPAP may be localized at thalamostriatal synapses. While SAPAP3 is the sole SAPAP that is highly expressed in the striatum, low levels of expression of other SAPAPs are detectable in striatum (3). Using quantitative real-time PCR, we measured mRNA abundance for each of the SAPAP family members in striatal tissue and found that SAPAP4 mRNA was the next most abundant (Figure S2 in Supplement 1). To determine whether SAPAP4 is present at thalamostriatal synapses of MSNs, we examined SAPAP4 immunostaining in striatal slices using vGluT2 as a marker for thalamic synaptic puncta. vGluT2 colocalizes with thalamostriatal terminals from certain intralaminar nuclei and does not colocalize with corticostriatal terminals (25-29). Punctate SAPAP4 immunostaining was readily detectable in striatum colocalizing with vGluT2 (WT: 30.0 ± 0.6 %, 20 regions; KO: 36.8 ± 1.2 %, 20 regions; Figure 4A, B). To determine whether SAPAP4 was circuit-selectively targeted to thalamostriatal but not corticostriatal synapses, we took advantage of co-cultured neuronal preparations to isolate and define the afferent source and to reduce the density of staining thereby increasing the specificity of colocalizing signal. Corticostriatal synapses are associated with vGluT1 and not vGluT2 whereas vGluT2 is a specific marker for some, but not all, thalamostriatal synapses (27-29). By co-culturing striatal tissue with either cortex or thalamus, we reproduced the expected divergent expression pattern of vGluTs in primary neuronal cultures (Figure 5A). Using the co-culture preparation, we found that, as predicted from tissue studies, vGluT2-positive puncta were present only on MSNs in thalamostriatal co-cultures. Corticostriatal co-cultures contained vGluT1- but not vGluT2-positive puncta. Note that vGluT1 signaling was detected in both types of co-cultures, consistent with prior results showing vGluT1 mRNA in some thalamic regions that project to striatum (27-29). Therefore, we used vGluT2 as a specific marker of thalamic terminals in thalamostriatal co-cultures and vGluT1 as a marker for cortical terminals in corticostriatal co-cultures. Using the corresponding vGluT marker for each culture type, we evaluated the co-localization of SAPAP4 and vGluT on MSN dendrites (identified by DARPP32 immunostaining). In thalamostriatal co-cultures, SAPAP4 was readily detected at vGluT2-positive puncta, while in corticostriatal co-cultures, there was no discernable SAPAP4 signal at vGluT1-positive puncta (thalamostriatal: vGluT2 and SAPAP4 colocalization/total vGluT2×100; 40.5 ± 2.4 %, 43 $DARPP32^+$ dendritic regions; corticostriatal: vGluT1 and SAPAP4 colocalization/total vGluT1×100; 0.7 ± 0.1 %, 57 $DARPP32^+$ dendritic regions; $p < 0.001$, Mann-Whitney; Figure 5B, C). These findings indicate that MSNs assemble postsynaptic structures in a circuit-specific manner, with SAPAP4 present at thalamostriatal synapses, but not corticostriatal synapses.

Discussion

In the present study, we show for the first time that the activity of excitatory synapses onto striatal MSNs is circuit-selectively altered in the *Sapap3* KO mouse model of obsessive-compulsive disorder. In explaining the basis for this functional divergence, we identify a novel difference in the postsynaptic molecular composition of corticostriatal and thalamostriatal synapses – SAPAP4 being present at thalamostriatal, but not corticostriatal, synapses. These observations advance both our understanding of the circuit basis for neuropsychiatric behaviors as modeled in mice and of properties that distinguish corticostriatal from thalamostriatal synapses. Because the OCD-like behaviors of *Sapap3* KO mice are known to derive from striatal excitatory synaptic dysfunction (7), our finding that thalamostriatal synapses are unaffected focuses attention on the corticostriatal circuit defects for its role in the OCD-like behaviors.

Functional and anatomical differences have been described between corticostriatal and thalamostriatal synapses (14-17). In this study, we identify a novel difference in molecular composition of the postsynaptic scaffold between cortical and thalamic synapses onto MSNs. Thalamostriatal synapses, but not corticostriatal synapses, contain SAPAP4. At present we cannot say whether the corollary is true, i.e. that SAPAP3 is present at corticostriatal but not thalamostriatal synapses, or whether the 3 isoform is targeted to both synapse types, since suitable SAPAP3 antibody reagents are not available. While it is known that there is great molecular diversity at synapses and that most synaptic proteins have multiple isoforms, there are relatively few examples of the principles guiding the distribution of the various isoforms. The few known examples generally concern neurotransmitter receptor subtypes that can be readily discriminated using electrophysiological and pharmacological techniques (30, 31). Our results reveal that MSNs have differential composition of SAPAP scaffold proteins at their postsynaptic densities according to neural circuitry. These results provide one of the first examples of principles guiding postsynaptic scaffold molecular diversity.

In the present study, both SP and SN MSNs of *Sapap3* KO mice had defects in corticostriatal but not thalamostriatal synaptic activity. It is interesting to consider why a reduction in mEPSC frequency was readily detectable in SN but not SP MSNs. One possibility for why a defect in mEPSC frequency was more easily detected in SN MSNs could be that corticostriatal synapses of *Sapap3* KO mice are more impaired in SN MSNs than SP MSNs. However, our corticostriatal eEPSC data suggest just the opposite (see Figure 1 in ref. 6). Another possibility is that thalamic inputs contribute to a greater proportion of synaptic activity in SP than SN MSNs. In mice, SP and SN MSNs have been reported to have similar proportions of structural synaptic contacts from cortex and thalamus (32). On the other hand, our results do indicate that a *functional bias* towards thalamostriatal synapses may exist in SP MSNs relative to SN MSNs. Our PPR data suggest a mechanism for this bias. Assuming that the observed PPR differences reflect relative differences in release probability, it is noteworthy, first, that in both SP and SN MSNs, PPR is lower for thalamostriatal synapses than corticostriatal synapses. This predicts that release probability may be higher in thalamostriatal synapses and would increase their relative contribution. Second, the difference in PPR between cortical and thalamic synapses is greater for SP than SN MSNs (T-S and C-S, $F = 141.72$, $p < 0.001$; T-S and C-S × SP and SN, $F = 7.10$, $p = 0.008$; three-way ANOVA; T-S, 66 cells; C-S, 100 cells; SP, 76 cells; SN, 90 cells; WT, 86 cells; KO, 80 cells), indicating that the effect of this functional bias favoring thalamostriatal synapses should be greater in SP than SN MSNs, consistent with our observations.

One of the promises of the application of molecular genetics to the study of behavior in animal models is the ability to precisely map behaviors onto neural circuits. *Sapap3* KO

mice have been useful in this effort, as the OCD-like constellation of behaviors can be rescued by *Sapap3* expression confined to the striatum (7). These experiments thus map the behaviors to striatum. OCD-like behaviors in *Sapap3* KO mice are further localized to excitatory synapses because SAPAPs are unique to excitatory synapses (3). However, among excitatory synapses in the striatum, there are two major sources – afferents from the cortex and thalamus. Striatal projection neurons receive inputs from both of these brain regions. Thus, either or both of these circuits might be responsible for driving OCD-like behaviors in *Sapap3* KO mice. Disentangling the relative contribution of corticostriatal and thalamostriatal circuits is difficult if not impossible using genetic techniques to manipulate SAPAP3 expression because inputs from both brain regions target the same postsynaptic MSN. Nevertheless, in this study, SAPAP biology serendipitously facilitated our understanding of the circuit dysfunction underlying OCD-like behaviors. In *Sapap3* KO mice, corticostriatal AMPAR synaptic transmission is impaired, while identical measures at thalamostriatal synapses are unaffected. These results are particularly relevant given recent advances in using circuit-based therapies for psychiatric disease. Deep brain stimulation for OCD is an active area of investigation and targeted regions include caudate (33). Our finding that only a subpopulation of striatal afferents is impaired in *Sapap3* KO mice indicate that targeting select striatal input fiber tracts may increase efficacy and decrease unnecessary modulation of unimpaired circuits. Moreover, because there are several mouse models with OCD-like behaviors (34), some of which also have defects in corticostriatal circuits (35-37), we now have an opportunity to determine the extent to which mouse models with similar behaviors share common circuit defects.

Supplementary Material

Refer to Web version on PubMed Central for supplementary material.

Acknowledgments

The authors would like to thank Ms. Samantha Tracy for outstanding technical support. N.C. was supported by grants from NINDS (NS054840, NS064577, and American Recovery and Reinvestment Act supplement), Tourette Syndrome Association, and NARSAD. C.E. and N.C. received support from the Esther and Joseph Klingenstein Fund and NIDA (DA031833). C.E. is an Alfred Sloan Foundation fellow. G.F. was supported by a grant from NIMH (MH081201), a Hartwell Individual Biomedical Research Award from The Hartwell Foundation, and a Simons Foundation Autism Research Initiative (SFARI) grant award. K.A. received support from an institutional T32NS051156 supported by NINDS.

References

1. Kim E, Naisbitt S, Hsueh YP, Rao A, Rothschild A, Craig AM, et al. GKAP, a novel synaptic protein that interacts with the guanylate kinase-like domain of the PSD-95/SAP90 family of channel clustering molecules. J Cell Biol. 1997; 136:669–678. [PubMed: 9024696]
2. Takeuchi M, Hata Y, Hirao K, Toyoda A, Irie M, Takai Y. SAPAPs. A family of PSD-95/SAP90-associated proteins localized at postsynaptic density. J Biol Chem. 1997; 272:11943–11951. [PubMed: 9115257]
3. Welch JM, Wang D, Feng G. Differential mRNA expression and protein localization of the SAP90/PSD-95-associated proteins (SAPAPs) in the nervous system of the mouse. J Comp Neurol. 2004; 472:24–39. [PubMed: 15024750]
4. Kim E, Sheng M. PDZ domain proteins of synapses. Nat Rev Neurosci. 2004; 5:771–781. [PubMed: 15378037]
5. Chen M, Wan Y, Ade K, Ting J, Feng G, Calakos N. Sapap3 deletion anomalously activates short-term endocannabinoid-mediated synaptic plasticity. J Neurosci. 2011; 31:9563–9573. [PubMed: 21715621]
6. Wan Y, Feng G, Calakos N. Sapap3 deletion causes mGluR5-dependent silencing of AMPAR synapses. J Neurosci. 2011; 31:16685–16691. [PubMed: 22090495]

7. Welch JM, Lu J, Rodriguiz RM, Trotta NC, Peca J, Ding JD, et al. Cortico-striatal synaptic defects and OCD-like behaviours in Sapap3-mutant mice. Nature. 2007; 448:894–900. [PubMed: 17713528]
8. Boardman L, van der Merwe L, Lochner C, Kinnear CJ, Seedat S, Stein DJ, et al. Investigating SAPAP3 variants in the etiology of obsessive-compulsive disorder and trichotillomania in the South African white population. Compr Psychiatry. 2011; 52:181–187. [PubMed: 21295225]
9. Ryu S, Oh S, Cho EY, Nam HJ, Yoo JH, Park T, et al. Interaction between genetic variants of DLGAP3 and SLC1A1 affecting the risk of atypical antipsychotics-induced obsessive-compulsive symptoms. Am J Med Genet B Neuropsychiatr Genet. 2011; 156B:949–959. [PubMed: 21990008]
10. Zuchner S, Wendland JR, Ashley-Koch AE, Collins AL, Tran-Viet KN, Quinn K, et al. Multiple rare SAPAP3 missense variants in trichotillomania and OCD. Mol Psychiatry. 2009; 14:6–9. [PubMed: 19096451]
11. Friedlander L, Desrocher M. Neuroimaging studies of obsessive-compulsive disorder in adults and children. Clin Psychol Rev. 2006; 26:32–49. [PubMed: 16242823]
12. Pennartz CM, Berke JD, Graybiel AM, Ito R, Lansink CS, van der Meer M, et al. Corticostriatal Interactions during Learning, Memory Processing, and Decision Making. J Neurosci. 2009; 29:12831–12838. [PubMed: 19828796]
13. Smith Y, Surmeier DJ, Redgrave P, Kimura M. Thalamic contributions to Basal Ganglia-related behavioral switching and reinforcement. J Neurosci. 2011; 31:16102–16106. [PubMed: 22072662]
14. Ding J, Peterson JD, Surmeier DJ. Corticostriatal and thalamostriatal synapses have distinctive properties. J Neurosci. 2008; 28:6483–6492. [PubMed: 18562619]
15. Dube L, Smith AD, Bolam JP. Identification of synaptic terminals of thalamic or cortical origin in contact with distinct medium-size spiny neurons in the rat neostriatum. J Comp Neurol. 1988; 267:455–471. [PubMed: 3346370]
16. Smeal RM, Gaspar RC, Keefe KA, Wilcox KS. A rat brain slice preparation for characterizing both thalamostriatal and corticostriatal afferents. J Neurosci Methods. 2007; 159:224–235. [PubMed: 16899300]
17. Smith Y, Raju DV, Pare JF, Sidibe M. The thalamostriatal system: a highly specific network of the basal ganglia circuitry. Trends Neurosci. 2004; 27:520–527. [PubMed: 15331233]
18. Villalba RM, Smith Y. Differential structural plasticity of corticostriatal and thalamostriatal axo-spinous synapses in MPTP-treated Parkinsonian monkeys. J Comp Neurol. 2011; 519:989–1005. [PubMed: 21280048]
19. Gong S, Zheng C, Doughty ML, Losos K, Didkovsky N, Schambra UB, et al. A gene expression atlas of the central nervous system based on bacterial artificial chromosomes. Nature. 2003; 425:917–925. [PubMed: 14586460]
20. Shuen JA, Chen M, Gloss B, Calakos N. Drd1a-tdTomato BAC transgenic mice for simultaneous visualization of medium spiny neurons in the direct and indirect pathways of the basal ganglia. J Neurosci. 2008; 28:2681–2685. [PubMed: 18337395]
21. Gerfen CR. The neostriatal mosaic: multiple levels of compartmental organization in the basal ganglia. Annu Rev Neurosci. 1992; 15:285–320. [PubMed: 1575444]
22. Kreitzer AC, Malenka RC. Striatal plasticity and basal ganglia circuit function. Neuron. 2008; 60:543–554. [PubMed: 19038213]
23. Ippolito DM, Eroglu C. Quantifying synapses: an immunocytochemistry-based assay to quantify synapse number. Journal of visualized experiments : JoVE. 2010
24. Goda Y, Stevens CF. Two components of transmitter release at a central synapse. Proc Natl Acad Sci U S A. 1994; 91:12942–12946. [PubMed: 7809151]
25. Fujiyama F, Kuramoto E, Okamoto K, Hioki H, Furuta T, Zhou L, et al. Presynaptic localization of an AMPA-type glutamate receptor in corticostriatal and thalamostriatal axon terminals. Eur J Neurosci. 2004; 20:3322–3330. [PubMed: 15610164]
26. Kaneko T, Fujiyama F, Hioki H. Immunohistochemical localization of candidates for vesicular glutamate transporters in the rat brain. J Comp Neurol. 2002; 444:39–62. [PubMed: 11835181]
27. Barroso-Chinea P, Castle M, Aymerich MS, Lanciego JL. Expression of vesicular glutamate transporters 1 and 2 in the cells of origin of the rat thalamostriatal pathway. J Chem Neuroanat. 2008; 35:101–107. [PubMed: 17826944]

28. Barroso-Chinea P, Castle M, Aymerich MS, Perez-Manso M, Erro E, Tunon T, et al. Expression of the mRNAs encoding for the vesicular glutamate transporters 1 and 2 in the rat thalamus. J Comp Neurol. 2007; 501:703–715. [PubMed: 17299752]
29. Graziano A, Liu XB, Murray KD, Jones EG. Vesicular glutamate transporters define two sets of glutamatergic afferents to the somatosensory thalamus and two thalamocortical projections in the mouse. J Comp Neurol. 2008; 507:1258–1276. [PubMed: 18181146]
30. Rubio ME, Wenthold RJ. Glutamate receptors are selectively targeted to postsynaptic sites in neurons. Neuron. 1997; 18:939–950. [PubMed: 9208861]
31. Toth K, McBain CJ. Afferent-specific innervation of two distinct AMPA receptor subtypes on single hippocampal interneurons. Nat Neurosci. 1998; 1:572–578. [PubMed: 10196564]
32. Doig NM, Moss J, Bolam JP. Cortical and thalamic innervation of direct and indirect pathway medium-sized spiny neurons in mouse striatum. J Neurosci. 2010; 30:14610–14618. [PubMed: 21048118]
33. de Koning PP, Figee M, van den Munckhof P, Schuurman PR, Denys D. Current status of deep brain stimulation for obsessive-compulsive disorder: a clinical review of different targets. Curr Psychiatry Rep. 2011; 13:274–282. [PubMed: 21505875]
34. Albelda N, Joel D. Current animal models of obsessive compulsive disorder: an update. Neuroscience. 2012; 211:83–106. [PubMed: 21925243]
35. Blundell J, Blaiss CA, Etherton MR, Espinosa F, Tabuchi K, Walz C, et al. Neuroligin-1 deletion results in impaired spatial memory and increased repetitive behavior. J Neurosci. 2010; 30:2115–2129. [PubMed: 20147539]
36. Peca J, Feliciano C, Ting JT, Wang W, Wells MF, Venkatraman TN, et al. Shank3 mutant mice display autistic-like behaviours and striatal dysfunction. Nature. 2011; 472:437–442. [PubMed: 21423165]
37. Shmelkov SV, Hormigo A, Jing D, Proenca CC, Bath KG, Milde T, et al. Slitrk5 deficiency impairs corticostriatal circuitry and leads to obsessive-compulsive-like behaviors in mice. Nature medicine. 2010; 16:598–602. 591p following 602.

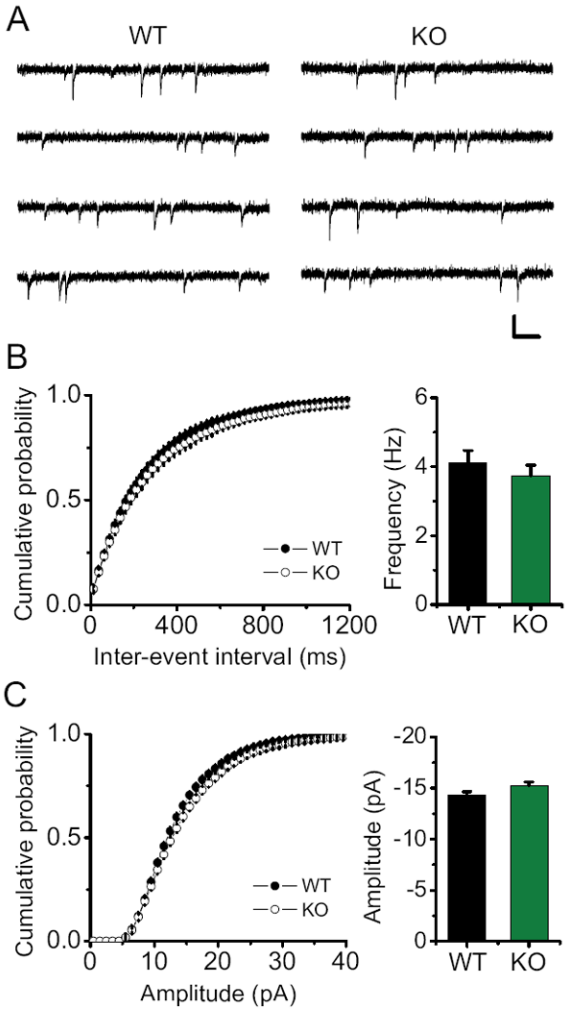

Figure 1.

Miniature EPSC events are unchanged in *Sapap3* KO striatopallidal MSNs. **(A)** Representative traces of mEPSC recordings from SP MSNs. Scale bars: 20 pA and 100 ms. **(B, C)** Neither frequency nor amplitude of mEPSCs is significantly changed in *Sapap3* KO SP MSNs.

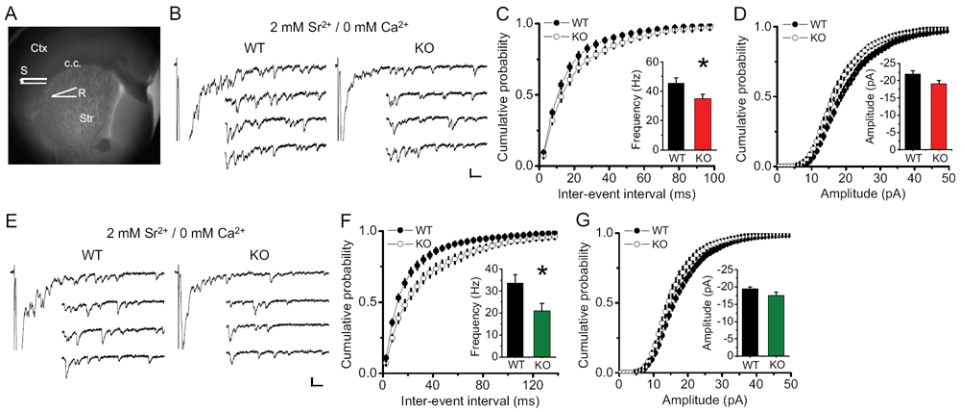

Figure 2.

Circuit-selective analysis is necessary to reveal quantal event defects in corticostriatal synaptic transmission of *Sapap3* KO SP MSNs. **(A)** Experimental recording paradigm for corticostriatal synapses. Ctx: cortex; c.c.: corpus callosum; Str: striatum; R: recording electrode; S; stimulating electrode. **(B)** Representative traces of corticostriatal qEPSC recordings in SN MSNs. Scale bars: 30 pA and 20 ms. **(C)** Frequency of corticostriatal qEPSCs is decreased in *Sapap3* KO SN MSNs. **(D)** No significant change in corticostriatal qEPSC amplitude of *Sapap3* KO SN MSNs is observed (WT, -21.9 ± 0.9 pA, 13 cells; KO, -19.1 ± 0.8 pA, 13 cells; $p = 0.054$, Mann-Whitney). **(E)** Representative traces of corticostriatal qEPSC recordings in SP MSNs. Scale bars: 30 pA and 20 ms. **(F)** Frequency of corticostriatal qEPSCs is decreased in *Sapap3* KO SP MSNs. **(G)** Amplitude of corticostriatal qEPSCs is normal in *Sapap3* KO SP MSNs.

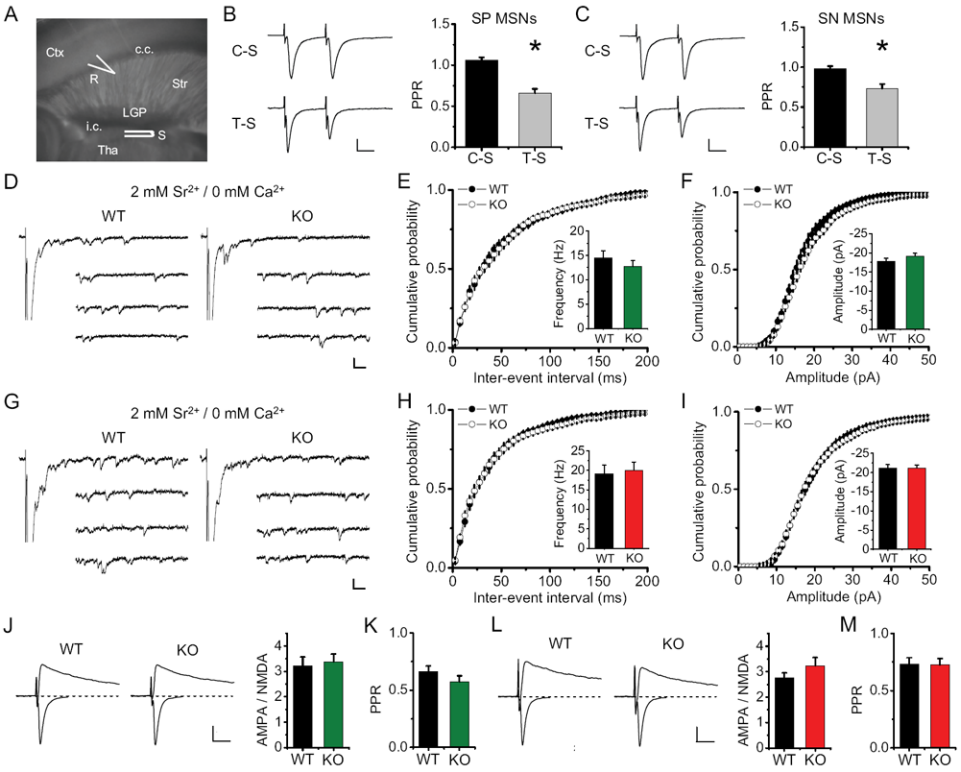

Figure 3.

SP and SN MSNs of *Sapap3* KO mice show no alterations in thalamostriatal synaptic transmission. **(A)** Experimental recording paradigm for thalamostriatal synapses. Ctx: cortex; c.c.: corpus callosum; Str: striatum; LGP: lateral globus pallidus; i.c.: internal capsule; Tha: thalamus; R: recording electrode; S; stimulating electrode. **(B, C)** Paired-pulse ratios (PPRs) are significantly different between corticostriatal and thalamostriatal synapses of both SP and SN MSNs. Representative traces are shown. Scale bars: 100 pA and 20 ms. **(D-I)** Frequency and amplitude of thalamostriatal qEPSCs are unchanged in *Sapap3* KO SP **(D-F)** and SN **(G-I)** MSNs. Representative traces are shown. Scale bars: 30 pA and 20 ms. **(J, L)** Thalamostriatal AMPAR/NMDAR ratio is normal in *Sapap3* KO SP **(J)** and SN **(L)** MSNs. Representative traces are shown. Scale bars: 100 pA and 20 ms. **(K, M)** Thalamostriatal PPRs are normal in *Sapap3* KO SP **(K)** and SN **(M)** MSNs.

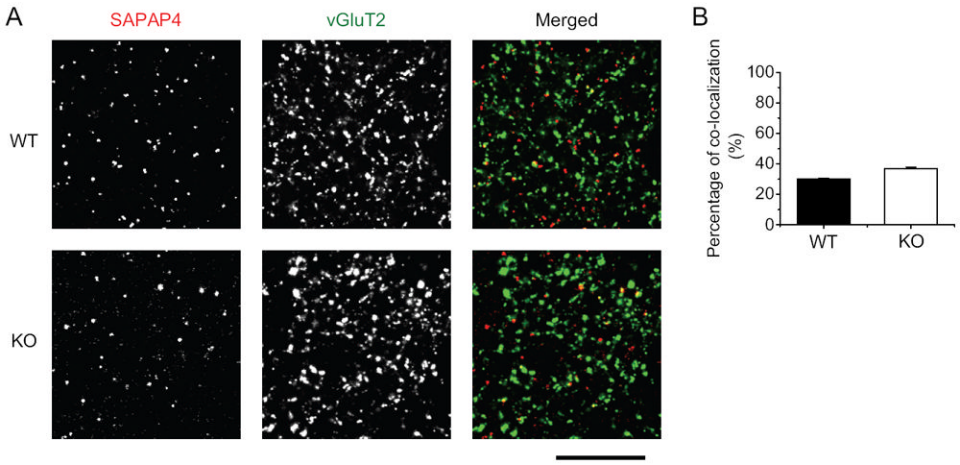

Figure 4.

Co-localization of SAPAP4 and vGluT2 in striatal brain slices. **(A)** SAPAP4 and vGluT2 immuno-fluorescence in the striatum of *Sapap3* WT and KO mice. Scale bar: 10 μm. **(B)** Percentage of SAPAP4 that colocalizes with vGluT2.

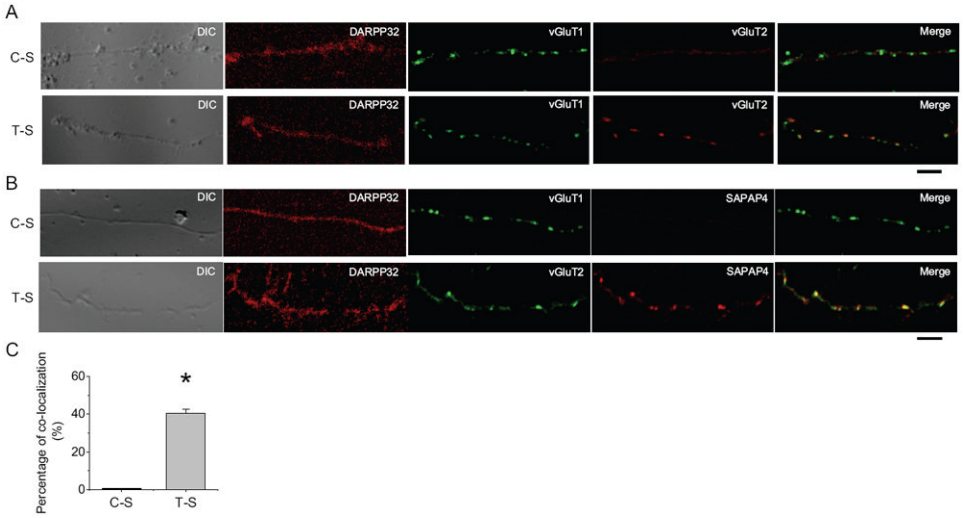

Figure 5.

SAPAP4 is present at thalamostriatal, but not corticostriatal, synapses. **(A)** vGluT1 and vGluT2 immuno-fluorescence on MSN dendrites in corticostriatal and thalamostriatal co-cultures. Scale bar: 4 μm. **(B)** vGluT1 or vGluT2 and SAPAP4 immuno-fluorescence on MSN dendrites in corticostriatal and thalamostriatal co-cultures. Scale bar: 4 μm. **(C)** Percentage of vGluT2 that colocalizes with SAPAP4 in thalamostriatal co-cultures is significantly higher than the percentage of vGluT1 that colocalizes with SAPAP4 in corticostriatal co-cultures.